JOURNAL OF GUIDANCE, CONTROL, AND DYNAMICS
Vol. 24, No. 1, January–February 2001

Three-Axes Missile Autopilot Design: From Linear to Nonlinear Control Strategies

Emmanuel Devaud*
Aerospatiale Matra Missiles, 92323 Châtillon CEDEX, France
Supelec, 91192 Gif-sur-Yvette, France
Jean-Philippe Harcaut†
Aerospatiale Matra Missiles, 92323 Châtillon CEDEX, France
and
Houria Siguerdidjane‡
Supelec, 91192 Gif-sur-Yvette, France

A three-axes skid-to-turn missile autopilot design is presented. The modeling is that of a missile developed by Aerospatiale Matra Missiles. Various control laws have been compared in order to estimate their potential and their applicability: classical linear time-invariant control and static and dynamic approximate input-output linearizing feedbacks. The robustness is studied, and the best results, in terms of stability, performance, and robustness, are shown to be obtained by using a special type of nonlinear dynamic control. The simulation results are explained using a table of comparison.

I. Introduction

CLASSICALLY, missile autopilots are designed using linear control approaches. Autopilot design has been studied in frequency domain[1] and/or by applying linear quadratic regulators.[2] In both cases, the plant is linearized around fixed operating points. Such methods lead to design linear time invariant (LTI) controllers for the LTI systems thus obtained. Operating points are, in general, defined by the triplet Mach number, altitude, and weight, which are considered as slowly varying parameters. Interpolation techniques may then be used to connect local regions around these operating points.

The main difficulties in missile autopilot design are known to result from the aerodynamic parameter uncertainties. Because the knowledge of the aerodynamic coefficients as well as their dependencies on some parameters[3] (e.g., angle of attack, side-slip angle, etc.) is very imprecise, the designed controller must not be sensitive to the variations of these coefficients. However, in spite of the wide literature on this subject, some problems still remain, for example, the degradation of the stability and performance for low Mach number and/or for high altitude due to low dynamic pressure.

In the last decade, the design of missile autopilot has been extensively studied using modern gain scheduling techniques[4–8] and robust control.[9,10] These methods are also based on local linearization.

Aerodynamic considerations dictated by new concepts, such as high maneuverability and stealthness, explicitly take into account the plant nonlinearities when designing a controller more and more necessary. Hence, linearizing techniques have become of great importance. In this context, nonlinear controllers based on the input-output feedback linearization of the missile dynamics have been developed[11–16] with eventually an outer loop in order to be robust with regards to uncertainties.[17,18] These techniques have also been studied for aircraft flight control.[19–21]

In the authors' previous works,[22–24] various nonlinear control laws have been elaborated, based on a missile model taken from the paper by Reichert.[25] This model is, however, a single-axis one, and the actuator is described by a first order differential equation.

This paper is a consideration of a three-axes model of a skid-to-turn missile developed by Aerospatiale Matra Missiles. Sensors and complete actuators modeling are also taken into account.

The paper is organized as follows. Section II describes the model of the missile. Since one of the objectives is to estimate the potential of nonlinear methods and their applicability level and in order to establish comparisons as well, we have first addressed a classical controller proportional integral in Sec. III. Section IV is devoted to the design of various linearizing control laws (approximate static and dynamic feedbacks). Section V describes a comparison performed between these various control strategies. The simulation results, which are obtained by using an industrial flight simulator corresponding to the real-world missile, are presented. The advantages and the drawbacks of each strategy are summarized in a comparison table. The paper ends with a conclusion.

II. Formulation of the Missile Problem

The aim of the problem is to force a missile to track a desired acceleration pattern generated by an outer loop, namely the guidance loop, and to stabilize the missile airframe at a given bank angle. The scheme is described in Fig. 1, where the word "missile" stands for the system composed of a skid-to-turn missile as well as the actuators, sensors, and various time delays.

The purposes of the autopilot are the following:

1) Compare the reference accelerations (for the center of mass) and roll angle to the actual measured normal accelerations and the bank angle, respectively, in order to estimate the corresponding tracking errors.

2) Generate the tail deflections that produce the angle of attack as well as the side-slip angle corresponding to a required maneuver, and ensure the tracking of the bank angle.

The missile model considered hereafter is a three-axes, highly nonlinear model of a skid-to-turn cruciform missile. For obvious reasons, the units used in the sequel have been normalized.

The tail-controlled missile is depicted in Figs. 2a and 2b, from which results the seven-dimensional state-space model

$$\dot{\alpha} = \frac{\cos(\alpha)}{V\cos(\beta)}\left(\frac{F_z}{m}\right) - p\cos(\alpha)\tan(\beta) + q - \frac{\sin(\alpha)}{V\cos(\beta)}\left(\frac{F_x}{m}\right) - r\sin(\alpha)\tan(\beta)$$

Received 17 February 1999; revision received 22 March 2000; accepted for publication 11 April 2000.

*Doctoral Student, Département Automatique, Plateau de Moulon; Research Engineer, Aerospatiale Matra Missiles, 2 rue Béranger, B.P. 84.

†Research Engineer, Systems Techniques Department, 2 rue Béranger, B.P. 84; jean-philippe.harcaut@missiles.aeromatra.com.

‡Professor, Département Automatique, Plateau de Moulon; houria.siguerdidjane@supelec.fr.

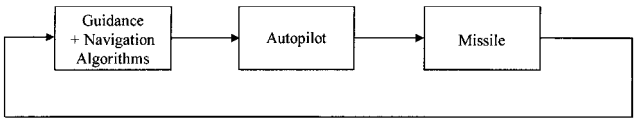

Fig. 1 Guidance–navigation–control loop.

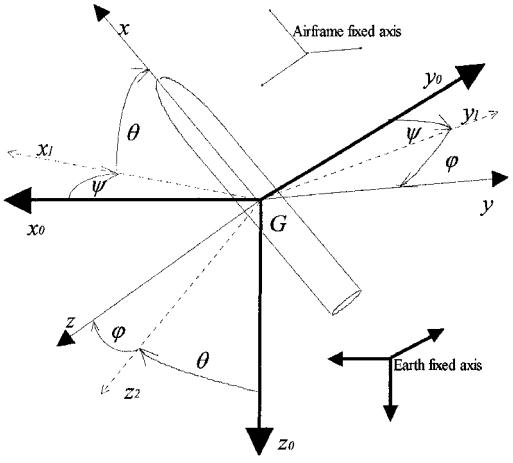

a) Azimuth, pitch, and bank angles

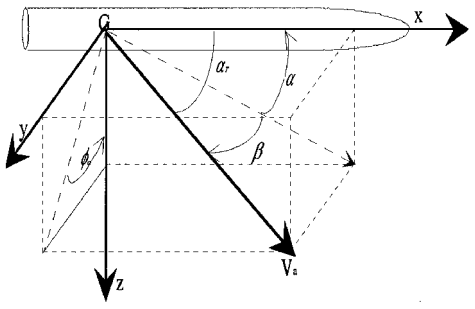

b) Angle of attack and side-slip angle

Fig. 2 Notations.

$$\dot{\beta} = \frac{\cos(\beta)}{V}\left(\frac{F_y}{m}\right) + p\sin(\alpha) - r\cos(\alpha) - \frac{\cos(\alpha)\sin(\beta)}{V}\left(\frac{F_x}{m}\right) - \frac{\sin(\alpha)\sin(\beta)}{V}\left(\frac{F_z}{m}\right)$$

$$\dot{p} = \frac{(I_y - I_z)}{I_x}qr + \frac{L_a}{I_x}, \qquad \dot{q} = \frac{(I_z - I_x)}{I_y}pr + \frac{M_a}{I_y}$$

$$\dot{r} = \frac{(I_x - I_y)}{I_z}qp + \frac{N_a}{I_z}, \qquad \dot{\phi} = p + \tan(\theta)[q\sin(\varphi) + r\cos(\varphi)]$$

$$\dot{\theta} = q\cos(\varphi) - r\sin(\varphi) \tag{1}$$

In these expressions, α is the angle of attack; β is the side-slip angle; θ and ϕ are the pitch and bank angles, respectively; and, p, q, and r are the roll, pitch, and yaw rotational rates, respectively. The constant parameters are the missile speed V; the missile mass m; and the mass moments of inertia I_x, I_y, and I_z about the x, y, and z axes, respectively. For the application under consideration, $I_y = I_z$ (due to the fact that the missile body is cruciform).

The system outputs are

$$Y = \begin{pmatrix} y_1 \\ y_2 \\ y_3 \end{pmatrix} = \begin{pmatrix} \varphi \\ \Gamma_y \\ \Gamma_z \end{pmatrix} = \begin{pmatrix} \varphi \\ F_y/m \\ F_z/m \end{pmatrix} \tag{2}$$

where φ, Γ_y, and Γ_z denote the roll angle and the lateral accelerations about y and z axes, respectively. The roll angle is estimated by the navigation algorithm.

Moreover, we have

$$F_x = F_{xa} - mg\sin(\theta), \qquad F_y = F_{ya} + mg\cos(\theta)\sin(\varphi)$$

$$F_z = F_{za} + mg\cos(\theta)\cos(\varphi) \tag{3}$$

where g denotes the acceleration of gravity.

The aerodynamic forces F_{xa}, F_{ya}, and F_{za} are the components of the force vector

$$\boldsymbol{F}_a = \begin{pmatrix} F_{xa} \\ F_{ya} \\ F_{za} \end{pmatrix} \tag{4}$$

Likewise, L_a, M_a, and N_a are the components of the moment vector

$$\boldsymbol{M}_a = \begin{pmatrix} L_a \\ M_a \\ N_a \end{pmatrix} \tag{5}$$

The vectors $\boldsymbol{F}_a$ and $\boldsymbol{M}_a$ are the aerodynamic forces and moments about the x, y, and z axes, which depend on the previously mentioned state variables as well as on the equivalent tail-fin deflections ξ, η, and ζ. The nonlinear aerodynamic coefficients used to determine these aerodynamic forces and moments are derived from wind tunnel measurements and are available through look-up tables, with associated multiplicative uncertainties. Therefore, their gradients with respect to the state variables are poorly known. Indeed, the look-up tables may be used to determine the analytical functions of α, β, M, ξ, η, ζ, etc., that are closest to the numerical values of the measured points[3] according to an appropriate criterion. Such a methodology would, for instance, lead to

$$L_a = f_1(\alpha_T)\sin(4\phi_a) + f_2(\alpha_T, \xi, \eta, \zeta) \tag{6}$$

for a given altitude and Mach number. The function $f_1(\alpha_T)$ is a polynomial function of its argument, and α_T and ϕ_a are the angles defined in Fig. 2b. But Eq. (6) must not hide the fact that the original sequence of measured points does not contain any information on the gradients of the aerodynamic functions.

The missile under consideration has unstable zero dynamics. This instability is caused mainly by the fact that the aerodynamic forces F_{ya} and F_{za} depend on the system input, namely, the tail fin deflections, in such a way that a tail fin deflection first generates a small force on the fin opposed to the desired acceleration.[23]

The modeling of the actuators is the same on each axis: it consists of second-order transfer functions with saturations on positions, speeds, and accelerations. In addition, sensors are modeled by appropriate transfer functions. The bandwith is sufficiently high to justify the fact that the sensors are not taken into account in the next controller designs. Time delays are added in order to take into account sampling and calculation delays.

III. Classical Controller Design

A linear control law is first designed for the missile, using classical aeronautical control rules,[1] based on Jacobian linearized models of each decoupled channel, and the resulting controller is validated on the whole nonlinear system. Consider the pitch channel shown in Fig. 3.

The airframe dynamics are second-order differential equations. The "high-order dynamics" block, which represents the actuators, sensors, and time delays, is represented by second-order equivalent dynamics, namely,

$$H_e(s) = \omega_e^2 \Big| \left(s^2 + 2\xi_e\omega_e s + \omega_e^2\right) \tag{7}$$

where $\xi = 0.7$ is the damping ratio and ω_e is the equivalent frequency for which the phase variation generated by the high frequency dynamics is -90 deg.

Designing a classical controller for this single-axis model is equivalent to looking for four gains l_0, l_1, l_2, and l_3. This, in turn, is equivalent to selecting gain margins for the loop opened at the actuator input point, and certain dynamics to the third-order equivalent closed-loop system, under some constraints, among which is the

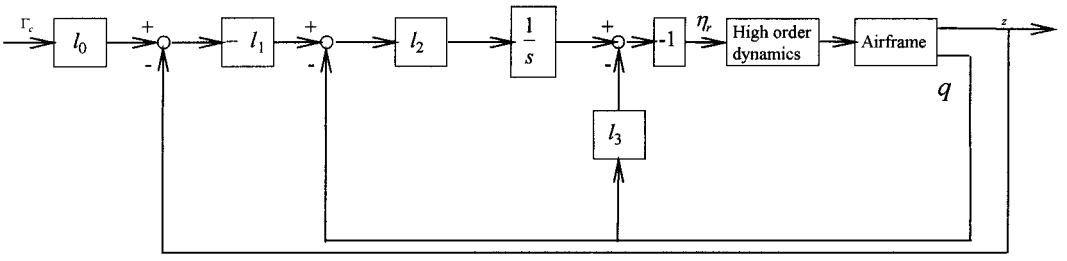

Fig. 3 Pitch channel.

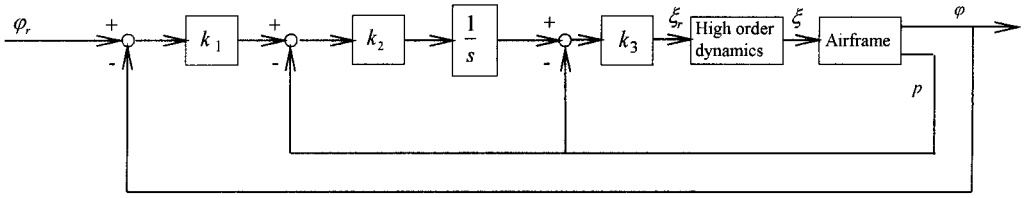

Fig. 4 Roll channel.

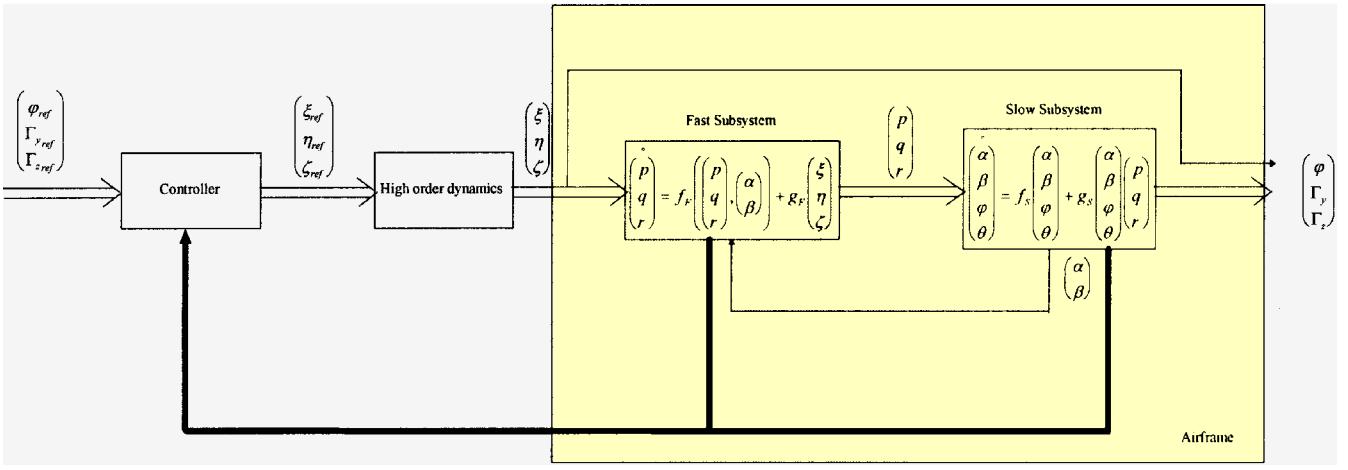

Fig. 5 Two-time scale separation.

bandwidth of the equivalent actuator.[1,2] The third-order dynamics are defined by the time constant τ, a damping ratio ξ, and a frequency ω (the latter is deduced from the three former parameters).

As a matter of fact, the procedure is nearly the same for the roll channel, except that the open loop involves an integrator; therefore, the gain k_0 is useless (Fig. 4).

IV. Nonlinear Control Laws

Three nonlinear control laws are proposed in the sequel. The first one is a static linearizing control law with two-time scale separation, whereas both the second and the third ones are dynamic linearizing control laws. The first control law corresponds to a basic application of linearizing techniques[26] combined with approximate linearization and time-scale separation. The two others rely on these techniques as well as on classical aeronautical knowledge because the methodology developed in the previous section is extended by fixing a given classical structure to the nonlinear controllers.

A. Static-State Feedback

The straightforward application of linearizing methodology leads to an unstable and unobservable manifold because, as already mentioned, the zero dynamics of the system are unstable. Hence it is necessary to use approximate feedback theory[27] in order to circumvent this difficulty.[12,22,23] Using approximate feedback theory leads to designing a linearizing control law on a modified model of the system, that is, on a model where the components of the aerodynamic forces do not depend on the tail-fin deflections.

Harcaut[12] showed that this design involves second derivatives of the aerodynamic coefficients with respect to the state variables. Because the aerodynamic coefficient functions have large uncertainties and are known through look-up tables only, the second-order gradients of these functions are unrealistic and should not be used. One attempt to overcome this difficulty proposed to use singular perturbations theory in order to separate the model into two different types of dynamics.[11] In this case, the control law is designed on some "fast" variables assuming that "slow" variables are nearly constant and are the commands of the fast subsystem, as illustrated in Fig. 5. As a matter of fact, the same argument is used to simply eliminate the equivalent high dynamics from the design model. It appears that including actuators with uncertain parameters in the linearization scheme may lead to adding high-pass dynamics (the inverse dynamics of the actuator) to the control law, which addition may not be satisfactory, especially with regard to noise considerations.

As a result of both points mentioned above, a two-time scale static linearizing control law was designed on an approximate model of the missile. Since the slow subsystem consisted of four ordinary first-order differential equations with relative degree {1, 1, 1} (see Ref. 26 for the classical definition hereafter recalled), and the fast one consisted of three ordinary first-order differential equations with relative degree {1, 1, 1}, the unobservable manifold is limited to the one described by the state variable θ (Ref. 12). Recall that the relative degree is a positive integer and, roughly speaking, is defined as the minimum number of times the output signal has to be differentiated for the control law to explicitly appear in the output derivative expression.

The resulting control law appears to have six degrees of freedom, corresponding to the six first-order time constants of each channel for both the slow (T_1, T_2, T_3) and the fast (τ_1, τ_2, τ_3) subsystems.

Tuning these time constants is not an easy task, but it can be done through considerations similar to those employed in the linear case:

1) The actuator dynamics must be significantly faster than the fast subsystem. By using the small gain theorem,[28] this condition can be expressed in terms of frequency magnitude conditions involving the transfer function of the neglected high dynamics and the transfer function of the "ideal" closed loop system.[29,30]

2) The fast subsystem must be significantly faster than the slow subsystem.

Finally, the time constants of the closed-loop subsystems are approximately equivalent to those of both loops in Sec. I. This equivalancy is logical because their choice is based on similar considerations.

Hence, the resulting control law is

$$u = \begin{pmatrix} \xi_{\text{ref}} \\ \eta_{\text{ref}} \\ \zeta_{\text{ref}} \end{pmatrix} = F_F + G_F \begin{pmatrix} \varphi_{\text{ref}} \\ \Gamma_{y_{\text{ref}}} \\ \Gamma_{z_{\text{ref}}} \end{pmatrix} \tag{8}$$

where ξ_{ref}, η_{ref}, and ζ_{ref} denote the input of the actuator; φ_{ref}, $\Gamma_{y_{\text{ref}}}$, and $\Gamma_{z_{\text{ref}}}$ are the reference inputs; and F_F and G_F denote the fast subsystem controller, and are related to the slow subsystem controller

$$G_F = g_F^{-1} G_S \operatorname{diag}(1/\tau_1, 1/\tau_2, 1/\tau_3) \tag{9}$$

$$F_F = g_F^{-1}\left[-f_F + G_S \operatorname{diag}(1/\tau_1, 1/\tau_2, 1/\tau_3) G_S^{-1}(u_S - F_S)\right] \tag{10}$$

In Eq. (10),

$$u_S = (p \quad q \quad r)^T \tag{11}$$

is the output of the fast subsystem as well as the command input of the slow subsystem. Likewise, F_S and G_S denote the slow subsystem controller obtained by a classical linearizing procedure that fixes the resulting dynamics to three first-order time constants T_1, T_2, and T_3. This procedure can be briefly summed up.

By denoting $X_S = (\alpha, \beta, \varphi, \theta)^T$ the slow state variables, substituting the notations in Fig. 5 yields

$$\dot{X}_S = f_S(X_S) + g_S(X_S) u_S \tag{12}$$

Straightforward calculations show that the time derivatives of the output can be related to u_S as follows:

$$\dot{Y} = \frac{\partial Y}{\partial X_S}[f_S(X_S) + g_S(X_S) u_S] \tag{13}$$

Equation (13) yields the so-called decoupling matrix of the slow subsystem:

$$\Delta_S = \frac{\partial Y}{\partial X_S} g_S(X_S) \tag{14}$$

which, for the application considered, is a full-rank matrix. Hence, it can easily be verified that

$$G_S = \Delta_S^{-1} \operatorname{diag}(1/T_1, 1/T_2, 1/T_3)$$

$$F_S = -\Delta_S^{-1}\left(\frac{\partial Y}{\partial X_S} f_S(X_S) + \operatorname{diag}\left(\frac{1}{T_1}, \frac{1}{T_2}, \frac{1}{T_3}\right) Y\right) \tag{15}$$

fixes the dynamics of the closed-loop slow subsystem as desired.

B. Dynamic-State Feedback

The previous control law is the most straightforward linearizing control law that can be applied to the missile (if no other assumption is made on the aerodynamic coefficients' gradients with respect to the state variables). As a drawback, that law turns out to be not so efficient because no effort was made to make it robust with respect to uncertainties. In order to make that control law robust, many improvements have been proposed, among which an extra outer loop, either linear[22] or nonlinear,[10] is the most frequently suggested. Nevertheless, one has to bear in mind that there is no theoretical guarantee on the margins or on the robustness of the original system, whatever may be the margin and robustness guaranteed by the outer-loop controller on the inner loop, as illustrated in Fig. 6.

In order to enhance the performance and robustness of the previous controller by using classical concepts on the feedback linearization context, dynamic feedback linearization has been applied to the missile.

1. *Dynamic Linearizing Autopilot, First Approach*

The first approach of the dynamic feedback presented here is the direct extension of the linear classical design (presented in Sec. III) to the static nonlinear control law (presented in Sec. IV.A). The idea is to keep the two-time scale structure, which is a common point between both these methods, and to fix second-order dynamics to the closed inner loop, that is, on the three fast state variables p, q, and r. This dynamic control law provides an extra degree of freedom on each channel, in which the degree of freedom is used to introduce an integral action on the fast variables.

Recall (Fig. 5) that, by denoting

$$X_F = (p, q, r)^T \tag{16}$$

$$X_S = (\alpha, \beta, \varphi, \theta)^T \tag{17}$$

one has for the fast subsystem

$$\dot{X}_F = f_F + g_F u \tag{18}$$

A dynamic state feedback can be deduced from Eq. (18)

$$u = -g_F^{-1}\left(f_F + 2\xi\omega X_F + \omega^2 \int (X_F - X_{\text{ref}})\, \mathrm{d}t\right) \tag{19}$$

where X_{ref} comes from the relationship imposed by the slow loop linearizing control, ξ is the damping ratio, and ω is the natural frequency of the closed-loop fast-subsystem-desired second-order dynamics. The control is indeed implemented through an integrator and is adapted to use measurements rather than model knowledge. Finally, Eq. (19) yields

$$u = -g_F^{-1}\left\{f_F + 2\xi\omega X_F + \omega^2 G_S^*\left(Y + \operatorname{diag}\left(\frac{1}{T_1}, \frac{1}{T_2}, \frac{1}{T_3}\right) \times \int (Y_{\text{ref}} - Y)\, \mathrm{d}t\right)\right\} \tag{20}$$

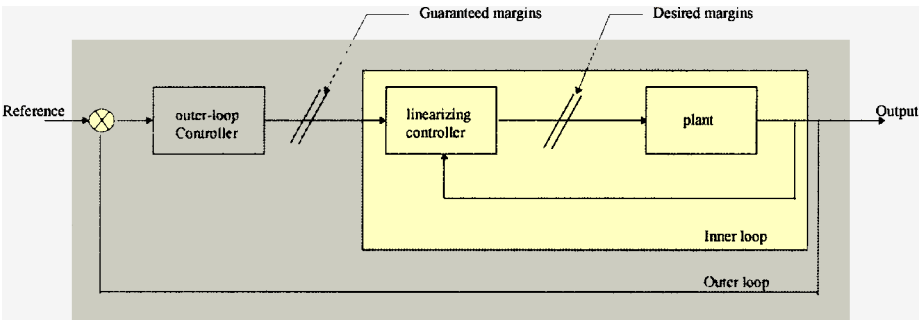

Fig. 6 Guaranteed margins.

where G_S^* is derived from the definition of the linearizing controller

$$\begin{pmatrix} p \\ q \\ r \end{pmatrix} = F_S^* + G_S^* \begin{pmatrix} \varphi_{\text{ref}} \\ \Gamma_{y_{\text{ref}}} \\ \Gamma_{z_{\text{ref}}} \end{pmatrix} \tag{21}$$

that transforms the slow subsystem into pure integrators.

2. Dynamic Linearizing Autopilot, Second Approach

An alternate version of the previous control law corresponds with an alternate version of the classical linear control law. In this scheme, the inner loop consists of a single gain, and the outer loop consists of a proportional integral law. On the one hand, the main advantage of this solution is that there is no steady-state error between the output and its reference signal. On the other hand, the main drawback is that an aerodynamic autopilot should first control the rotational rates in order to be efficient rather than to control by force. Controlling the rotational rates is all the more useful as the unstable zeros become more important (for instance, at low Mach number or high altitude).

Suppose again that the same dynamics are fixed on each channel (characterized by a first-order constant τ for each channel of the fast subsystem, a damping ratio ξ, and a natural frequency ω for the slow subsystem). A dynamic control law is first designed on the slow subsystem, according to the asymptotic output tracking problem methodology,[24,26] in order to fix the second-order dynamics of the closed-loop subsystem, even if a static-state feedback would be enough. A static-state feedback is thus designed on the fast subsystem, according to Sec. IV.A.

Finally, it yields

$$u = -g_F^{-1}\left\{ f_F + \frac{1}{\tau}\left(X_F + F_S^* + 2\xi\omega G_S^*(Y_{\text{ref}} - Y) + \omega^2 \int G_S^*(Y_{\text{ref}} - Y)\, \mathrm{d}t \right)\right\} \tag{22}$$

where, once again, G_S^* and F_S^* come from the definition of the linearizing controller

$$\begin{pmatrix} p \\ q \\ r \end{pmatrix} = F_S^* + G_S^* \begin{pmatrix} \varepsilon_{\varphi_{\text{ref}}} \\ \varepsilon_{y_{\text{ref}}} \\ \varepsilon_{z_{\text{ref}}} \end{pmatrix} \tag{23}$$

that transforms the slow subsystem into a chain of two pure integrators on each channel. In Eq. (23), the reference inputs are the tracking errors

$$\varepsilon_{\varphi_{\text{ref}}} = \varphi - \varphi_{\text{ref}}, \qquad \varepsilon_{y_{\text{ref}}} = \Gamma_y - \Gamma_{y_{\text{ref}}}, \qquad \varepsilon_{z_{\text{ref}}} = \Gamma_z - \Gamma_{z_{\text{ref}}} \tag{24}$$

V. Simulation Results

A. Necessity of an Observer

One should notice that the angle of attack α and the side-slip angle β are not available through measurements. An observer is then necessary. Devaud et al.[23] have shown that a simple quadratic observer can be designed straightforwardly for the single-axis case. Under some simplifying assumptions, an efficient quadratic observer may be obtained using a similar procedure.

Suppose that the state-space model equation is expressed in the following simplified way:

$$\begin{aligned} \dot{\alpha} &= F_z/mV - \beta p + q - (\alpha/V)\Gamma_x \\ \dot{\beta} &= F_y/mV + \alpha p - r - (\beta/V)\Gamma_x \end{aligned} \tag{25}$$

and suppose also that F_y depends on β only and F_z depends on α only.

Remark: The terms $\alpha\Gamma_x$ and $\beta\Gamma_x$ may be considered as higher-order terms with respect to α and β when the speed V is constant with respect to time, and, therefore, be neglected.

Hence the following observer

$$\begin{pmatrix} \dot{\hat{\alpha}} \\ \dot{\hat{\beta}} \end{pmatrix} = \begin{pmatrix} F_z(\hat{\alpha})/mV - \hat{\beta}p + q - (\hat{\alpha}/V)\Gamma_x \\ F_y(\hat{\beta})/mV + \hat{\alpha}p - r - (\hat{\beta}/V)\Gamma_x \end{pmatrix} + K\begin{pmatrix} \Gamma_z(\hat{\alpha}) - \Gamma_z(\alpha) \\ \Gamma_y(\hat{\beta}) - \Gamma_y(\beta) \end{pmatrix} \tag{26}$$

is shown to be an efficient quadratic observer, even for a diagonal K matrix

$$K = \text{diag}(k_1, k_2) \tag{27}$$

By setting

$$\delta\alpha = \hat{\alpha} - \alpha, \qquad \delta\beta = \hat{\beta} - \beta \tag{28}$$

$$V(\delta\alpha, \delta\beta) = \delta\alpha^2 + \delta\beta^2 \tag{29}$$

one obtains

$$\begin{aligned} \dot{V}(\delta\alpha, \delta\beta) &= 2(\hat{\alpha} - \alpha)[\Gamma_z(\hat{\alpha}) - \Gamma_z(\alpha)](1/V + k_1) \\ &\quad - (\hat{\alpha} - \alpha)^2(\Gamma_x/V) + 2(\hat{\beta} - \beta)[\Gamma_y(\hat{\beta}) - \Gamma_y(\beta)](1/V + k_2) \\ &\quad - (\hat{\beta} - \beta)^2(\Gamma_x/V) \end{aligned} \tag{30}$$

Through an appropriate choice of parameters k_1 and k_2, $V(\delta\alpha, \delta\beta)$ is a quadratic Lyapunov function because $\Gamma_z(\hat{\alpha})$ and $\Gamma_y(\hat{\beta})$ are decreasing functions of their arguments.

B. Normalized Step Responses for Various Accelerations on the z-axis (No Uncertainty)

The first result presented hereafter is a set of responses for various z-axis acceleration references while the y-axis reference is maintained equal to zero value, and the bank-angle reference is maintained equal to its nominal value. This reference configuration is considered to be a difficult one because it may induce roll divergence for high values of the angle of attack.

Figures 7a and 7b correspond to the linear classical controller. Note that whereas normalized z-axis acceleration seems satisfactory, the bank angle starts diverging for large values of the z-axis acceleration reference. This bank angle is the well-known "induced bank-angle," due to unbalanced actions by means of the acting moments on the missile according to Eq. (6). Note also that the overshoot magnitude depends on the acceleration reference.

For each of the linearizing control laws determined in Sec. IV, the induced bank angle phenomenon does not appear. Simulation results are quite similar for both static and first approach of the dynamic linearizing controller when no perturbation and uncertainty are added. For the sake of brevity, static-state feedback results are given here only (Figs. 8a and 8b).

The second approach of the dynamic linearizing control results in a difficult tradeoff between the settling time and the overshoot, as shown in Figs. 9a and 9b, due to the presence of a static-state controller in the inner loop that leads, in this case, to these less satisfactory responses.

C. Responses for a Given Acceleration Pattern for the Uncertain System

Section V.B shows that the first objective of the linearizing controller is reached: The input-output relationship is almost linear, the induced-roll angle does not appear anymore, and there is no variation in the overshoot. However, the robustness with respect to uncertainties needs to be studied. To this end, various aerodynamic uncertainties have been considered. Each aerodynamic coefficient is

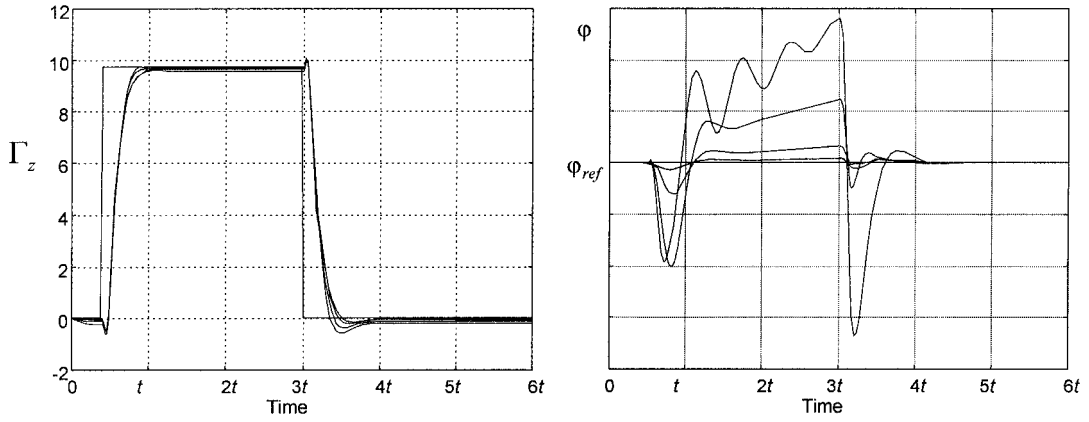

a) Normalized z-axis acceleration **b) Bank angle**

Fig. 7 Classical controller with various z-axis reference magnitudes.

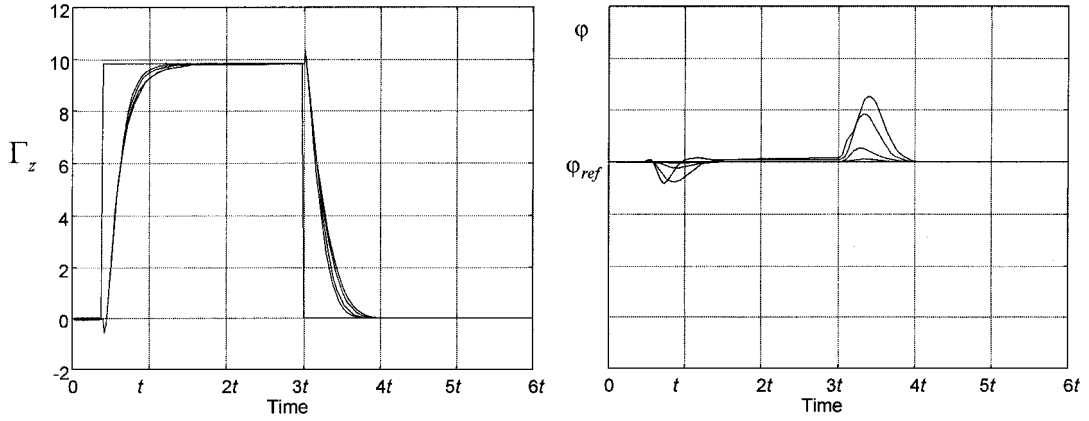

a) Normalized z-axis acceleration **b) Bank angle**

Fig. 8 Static linearizing controller with various z-axis reference magnitudes.

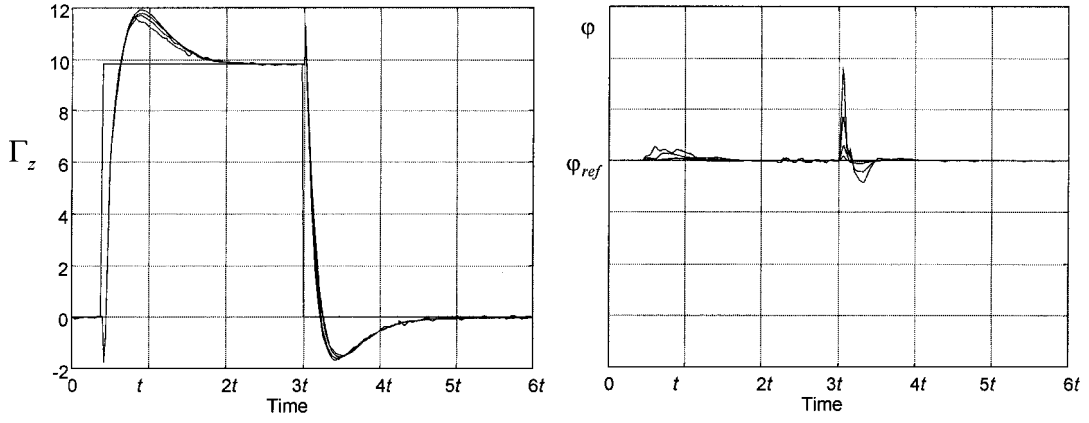

a) Normalized z-axis acceleration **b) Bank angle**

Fig. 9 Dynamic linearizing controller (case 2) with various z-axis reference magnitudes.

characterized by some random uncertainties described by a type of distribution law. This law may be a normal distribution function or a uniform one. Each distribution function is characterized by specific parameters (mean, variance, etc.) that come from measurements.

Simulations have been performed by introducing randomly generated perturbation terms on each aerodynamic coefficient simultaneously. These results, together with the nominal (unperturbed) ones, are presented in Figs. 10a and 10b for the nonlinear dynamic controller (case 1). They are quite satisfactory, in comparison, for instance, with those obtained by using the static nonlinear control law (Figs. 11a and 11b). In the latter case, the steady-state error may become quite large, together with the settling time.

D. Brief Qualitative Controller Comparison: from Linear to Nonlinear

Table 1, composed of four columns, summarizes the studied approaches. Various aspects are reported for each control law:

1) The second column, concerning the complexity, displays the existence of algorithms for the implementation and choice of the control law parameters.

2) The next column concerns the degrees of freedom, that is, the number of such parameters.

3) The last column sums up simulation results: stability and performance of the nominal closed-loop system, as well as robustness with respect to aerodynamical uncertainties.

Table 1 Comparison of six control strategies

Control strategy	Complexity	Degrees of freedom	Simulation results
Linear controller (Fig. 7)	Classical linear knowledge	3/channel (integral action)	Induced bank angle for high angle of attack Robustness with respect to uncertainties
Classical linearizing feedback	Linearization methodology	2/channel	Unobservable: unstable manifold of dimension 5 Discarded
Approximate feedback, no time scale separation, and static feedback	Linearization methodology	2/channel	Unrealistic Discarded
Approximate feedback, two-time scale separation, and static feedback (Figs. 8 and 11)	Classical knowledge + linearization methodology	2/channel	No induced bank angle No robustness with respect to uncertainties
Approximate feedback, two-time scale separation, and dynamic feedback 1 (Fig. 10)	Classical know-how + linearization methodology	3/channel (integral action)	No induced bank angle Robustness with respect to uncertainties
Approximate feedback, two-time scale separation, and dynamic feedback 2 (Fig. 9)	Classical knowledge, linearization methodology	3/channel (integral action)	No induced bank angle Robustness with respect to uncertainties Difficult tradeoff overshoot settling time

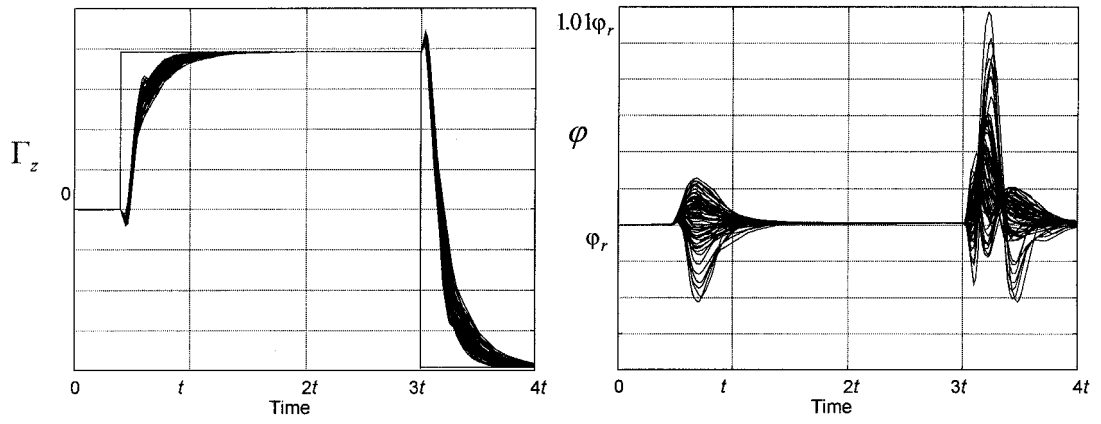

a) z-axis acceleration b) Bank angle

Fig. 10 Dynamic linearizing controller (case 1) with uncertain aerodynamic coefficients.

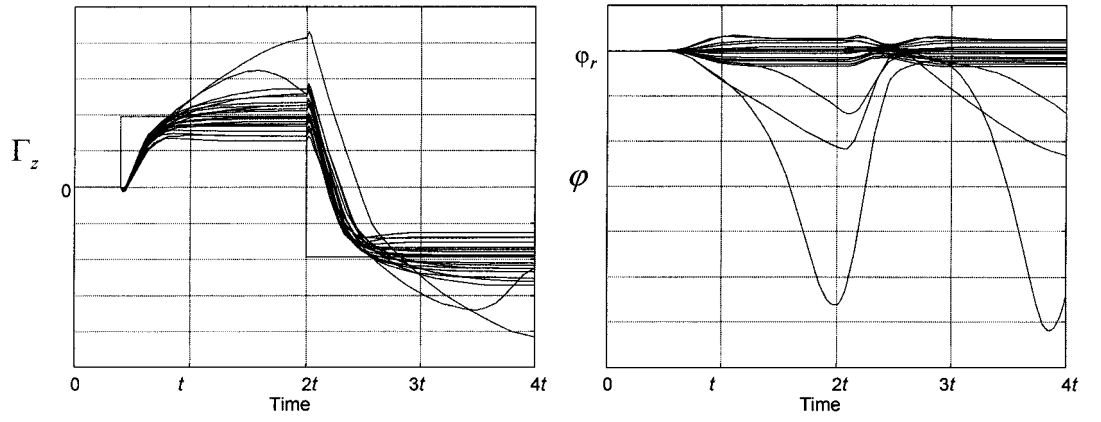

a) z-axis acceleration b) Bank angle

Fig. 11 Static linearizing controller with uncertain aerodynamic coefficients.

VI. Conclusion

In this paper, various methods have been presented for controlling a three-axes highly maneuverable missile. Our choice has been oriented by the industrial context. The necessity of increasing missile performances and flight range has motivated new investigations in order to estimate not only the potential of recent theoretical control methods, but also their application level, in order to meet the industrial demands. These investigations have led us to design various control laws, from linear to nonlinear and from static to dynamic, in order to establish comparisons according to various criteria, among which are stability and performance on the one hand, and complexity and degrees of freedom on the other. This comparison shows that the best tradeoff between the required criteria is the linearizing control law that reproduces the linear scheme, namely, a two-cascaded structure with an integral action in the inner loop, with some improvements due to its nonlinear character.

References

[1]Nesline, F. W., and Nabbefeld, N. C., "Design of Digital Autopilots for Homing Missiles," *AGARD Flight Mechanics Panel Symposium*, 1979, pp. 29-1–29-14.

[2]Nesline, F. W., Wells, B. H., and Zarchan, P., "A Combined Optimal/Classical Approach to Robust Missile Autopilot Design," *AIAA Guidance and Control Conference*, AIAA, New York, 1979, pp. 265–280.

[3]Oh, Y. H., "Three Dimensional Interpolation Method for Missile Aerodynamics," AIAA Paper 89-0481, 1989.

[4]Scorletti, G., "Approche Unifiée de l'Analyse et de la Commande par Formulation LMI," Ph.D. Dissertation, Univ. Paris XI, Orsay, France, 1997.

[5]Shamma, J. S., and Cloutier, J. R., "Gain Scheduled Missile Autopilot Design Using Linear Parameter Varying Transformation," *Journal of Guidance, Control, and Dynamics*, Vol. 16, No. 2, 1993, pp. 256–263.

[6]Nichols, R. A., Reichert, R. T., and Rugh, W. J., "Gain Scheduling for H_∞ Controllers: A Flight Control Example," *IEEE Transactions on Control, Systems, and Technologies*, Vol. 1, No. 2, 1993, pp. 69–78.

[7]Rugh, W. J., and Jackson, P. B., "Analysis of Gain Scheduling for the Three-Loop Autopilot Structure," Applied Physics Lab., Johns Hopkins Univ. TR JHU/ECE 94-02, 1994.

[8]Wu, F., Packard, A., and Balas, G., "LPV Control Design for Pitch Axis Missile Autopilots," *34th IEEE Conference on Decision and Control*, IEEE Publications, Piscataway, NJ, 1995, pp. 188–191.

[9]Fromion, V., "Une Approche Incrémentale de la Robustesse non Linéaire: Application au Domaine de l'Aéronautique," Ph.D. Dissertation, Univ. Paris XI, Orsay, France, 1995.

[10]Hull, R. A., Schumacher, D., and Qu, Z., "Design and Evaluation of Robust Nonlinear Missile Autopilots from a Performance Perspective," *American Control Conference*, 1995, pp. 189–193.

[11]Menon, P. K., Badget, M. E., Walker, R. A., and Duke, E. L., "Nonlinear Flight Test Trajectory Controllers for Aircraft," *Journal of Guidance, Control, and Dynamics*, Vol. 10, No. 1, 1987, pp. 67–72.

[12]Harcaut, J. P., "Nonlinear Control of Missiles Through a Geometric Approach," *Lecture Notes in Control and Information Sciences*, Vol. 144, Springer-Verlag, Berlin, 1990, pp. 27–36.

[13]Harcaut, J. P., "Commande non Linéaire Appliquée au Pilotage d'un Engin," Ph.D. Dissertation, Ecole Nationale Supérieure d'Aéronautique et de l'Espace, Toulouse, France, 1991.

[14]Fossard, A. J., Foisneau, J., and Hun Huynh, T., "Optimisation Approchée en Boucle Fermée des Systèmes Non Linéaires par la Méthodologie des Perturbations Singulières," *Systèmes non Linéaires*, Vol. 3, edited by A. J. Fossard and D. Normand-Cyrot, Masson, Paris, 1993, pp. 173–229.

[15]Menon, P. K., and Yousefpor, M., "Design of Nonlinear Autopilots for High Angle of Attack Missile," AIAA Paper 96-3913, 1996.

[16]Menon, P. K., Iragavarapu, V. R., and Ohlmeyer, E. J., "Nonlinear Missile Autopilot Using Time Scale Separation," AIAA Paper 96-3765, 1997.

[17]Ryu, J. H., Park, C. S., and Tahk M. J., "Plant Inversion of Tail-Controlled Missile," AIAA Paper 97-3766, 1997.

[18]Snell, S. A., and Stout, P. W., "Robust Longitudinal Control Design Using Dynamic Inversion and Quantitative Feedback Theory," *Journal of Guidance, Control, and Dynamics*, Vol. 20, No. 5, 1997, pp. 933–940.

[19]Snell, S. A., Enns, D. F., and Garrard, W. L., "Nonlinear Inversion Flight Control for a Supermaneuverable Aircraft," *Journal of Guidance, Control, and Dynamics*, Vol. 15, No. 4, 1992, pp. 976–984.

[20]Reiner, J., Balas, G. J., and Garrard, W. L., "Robust Dynamic Inversion for Control of Highly Maneuverable Aircraft," *Journal of Guidance, Control, and Dynamics*, Vol. 18, No. 1, 1995, pp. 18–24.

[21]Reiner, J., Balas, G. J., and Garrard, W. L., "Flight Control Design Using Robust Dynamic Inversion and Time Scale Separation," *Automatica*, Vol. 32, No. 11, 1996, pp. 1493–1504.

[22]Devaud, E., Siguerdidjane, H., and Font, S., "Some Control Strategies of High Angle of Attack Missile Autopilot," *Control Engineering Practice International Federation of Automatic Control Journal* (to be published).

[23]Devaud, E., Siguerdidjane, H., and Font, S., "Nonlinear Dynamic Autopilot Design for the Non Minimum Phase Missile," *37th IEEE Conference on Decision and Control*, IEEE Publications, Piscataway, NJ, 1998, pp. 4691–4696.

[24]Siguerdidjane, H., and Devaud, E., "Nonlinear Missile Autopilot Design Based on Angle of Attack Normal Form," *European Journal of Control*, Vol. 6, No. 2, 2000, pp. 154–164.

[25]Reichert, R. T., "Dynamic Scheduling of Modern-Robust-Control Autopilot Design for Missiles," *IEEE Control System Magazine*, Vol. 12, No. 5, 1992, pp. 35–42.

[26]Isidori, A., *Nonlinear Control Systems*, Springer-Verlag, Berlin, 1989.

[27]Hauser, J., Sastry, S., and Meyer, G., "Nonlinear Controller Design for Slightly Non Minimum Phase System: Application to V/STOL Aircraft," *Automatica*, Vol. 28, No. 4, 1992, pp. 665–679.

[28]Zames, G., "On the Input-Output Stability of Time Varying Nonlinear Feedback Systems, Part I: Conditions Derived Using Concepts of Loop Gain, Conicity, and Positivity," *IEEE Transactions on Automatic Control*, Vol. 11, No. 2, 1966, pp. 228–238.

[29]Enns, D., Bugajski, D., Hendrick, R., and Stein, G., "Dynamic Inversion: An Evolving Methodology for Flight Control Design," *International Journal of Control*, Vol. 59, No. 1, 1994, pp. 71–91.

[30]Chao, A., Athans, M., and Stein, G., "Stability Robustness to Unstructured Uncertainty for Nonlinear Systems Under Feedback Linearization," *33rd IEEE Conference on Decision and Control*, IEEE Publications, Piscataway, NJ, 1994, pp. 573–578.